promoting access to White Rose research papers

Universities of Leeds, Sheffield and York
http://eprints.whiterose.ac.uk/

This is an author produced version of a paper published in **Nanotechnology.**

White Rose Research Online URL for this paper:
http://eprints.whiterose.ac.uk/8571/

Published paper
Zhang, Y.H., Chen, Y.B., Zhou, K.G., Liu, C.H., Zeng, J., Zhang, H.L. and Peng, Y. (2009) *Improving gas sensing properties of graphene by introducing dopants and defects: a first-principles study.* Nanotechnology, 20 (18). Art. No.185504.
http://dx.doi.org/10.1088/0957-4484/20/18/185504

White Rose Research Online
eprints@whiterose.ac.uk

Improving gas sensing properties of graphene by introducing dopant and defect: a first-principles study

Yong-Hui Zhang[1], Ya-Bin Chen[1], Kai-Ge Zhou[1], Cai-Hong Liu[1], Jing Zeng[1], Hao-Li Zhang[1]* and Yong Peng[2]

[1]State Key Laboratory of Applied Organic Chemistry, College of Chemistry and Chemical Engineering, Lanzhou University, Lanzhou, 730000, China

[2]Department of Engineering Materials, Sheffield University, Sheffield, S1 3JD, UK

*Email: Haoli.Zhang@lzu.edu.cn

Abstract

The interactions between four different graphenes (including pristine, B or N doped and defective graphenes) and small gas molecules (CO, NO, NO_2 and NH_3) were investigated by using density functional computations to exploit their potential applications as gas sensors. The structural and electronic properties of the graphene-molecule adsorption adducts are strongly dependent on the graphene structure and the molecular adsorption configuration. All the four gas molecules show much stronger adsorption on the doped or defective graphenes than that on the pristine graphene. The defective graphene shows the highest adsorption energy with CO, NO and NO_2 molecules, while the B-doped graphene gives the tightest binding with NH_3. Meanwhile, the strong interactions between the adsorbed molecules and the modified graphenes induce dramatic changes to graphene's electronic properties. The transport behavior of a gas sensor using B-doped graphene shows a sensitivity two orders of magnitude higher than that of pristine graphene. This work reveals that the sensitivity of graphene based chemical gas sensors could be drastically improved by introducing appropriate dopant or defect.

1. Introduction

The successful synthesis of graphene (a single atomic layer of graphite sheet) and experimental observation of Dirac charge carries properties in graphene-based devices [1] have awakened an enormous interest in this two-dimensional material. Due to its unique structural, mechanical and electronic properties, graphene becomes an important candidate for numerous potential applications, ranging from composites [2, 3], gas sensors [4, 5], spintronic devices [6] and transparent electrodes for light emitting diodes and photovoltaics [7-9]. Graphene-based electronics should benefit from its exceptional high mobility of charge carriers high stability. Moreover, recent researches have demonstrated that various nanometre-size structures can be carved from graphene sheet to make a single-electron-transistor (SET) circuitry [10], which open new ways of fabrication novel nanoelectronics. Similar to carbon nanotubes [11-15], experimental and theoretical researches have shown that graphene can be used as sensing materials to detect various molecules, ranging from gas phase molecules to some small bioactive molecules [4, 16-18]. The simplest graphene-based sensor detects the conductivity change upon adsorption of analyte molecules. The change of conductivity could be attributed to the changes of charge carrier concentration in the graphene induced by adsorbed gas molecules. It has been proposed that such device may be capable of detecting individual molecule [11].

To fully exploit the possibilities of graphene sensors, it is important to understand the interaction between the graphene surface and the adsorbed molecules. Theoretical studies have been conducted to investigate the adsorption of small molecules on graphene. Most of the previous work focused on perfect graphene, and predicted relative low adsorption energies in comparison with the essential requirement of gas sensing applications [15, 19-24]. In reality, the graphene sheets prepared by the available fabrication methods are likely to have many defects. Besides, graphene could be deliberately or accidentally doped by non-carbon elements. To date, the number of studies on the effects of

dopants and defects on the sensing properties of graphene is surprisingly small.

In this work we report a first-principles simulation of the interactions between several small molecules and various graphene sheets. The model systems are carefully chosen to cover several basics issues. The gas molecules, CO, NO, NO_2 and NH_3, are all of great practical interests for industrial, environmental and medical applications. Meanwhile, NO_2 and NH_3 represent typical electron acceptor and donor, which may undergo charge transfer with graphene. The graphenes are doped by boron and nitrogen atoms, representing the most widely used p and n type dopants. For the defective graphene, only one defect containing a single missing atom in each super cell is considered for reducing complexity. Structural perfect graphene is also studied for comparison. The purpose of this work is to gain fundamental insights to the influence of adsorbed molecules on the electronic properties of different graphenes, and how these effects could be used to design more sensitive gas sensing devices.

2. Computational methods

The densitiy functional theory (DFT) calculations were performed with CASTEP [25] using ultrasoft pseudopotential, plane-wave basis and periodic boundary conditions. The local density approximation (LDA) with CA-PZ functional, and a 240 eV cut-off energy for the plane-wave basis set were used in all relaxation process. Each simulated system under investigation consisted of a 12.30×12.30×10 Å graphene super cell (50 C atoms) with a single molecule adsorbed in the center region (figure 1). The distance between adjacent graphene layers was kept as 10 Å. The *k*-point was set to 9×9×1 for the Brillouin zone integration. The structural configurations of the isolated graphenes were optimized through fully relaxing the atomic structures. With the same super cell and *k*-point samplings, the configurations of the molecule-graphene systems were optimized through fully relaxing the atomic structures until the remaining forces were smaller than 0.01 eV/Å. The adsorption energy of small molecule on graphene was calculated as：

$$E_{ad} = E_{(molecule+graphene)} - E_{(graphene)} - E_{(molecule)} \quad (1)$$

where $E_{(molecule+graphene)}$, $E_{(graphene)}$ and $E_{(molecule)}$ are the total energies of the relaxed molecule on

graphene system, graphene and the molecule, respectively. For the density of state (DOS) calculation, the *k*-point was set to 9×9×1 to achieve high accuracy.

In literature, GGA and LDA are two common methods used in the investigation on nanomaterials. As indicated by the previous theoretical calculations [20, 26], GGA methods tend to underestimate the adsorption energies. For example, GGA suggested that almost no interaction between two graphene layers. In contrast, LDA appeared to be more appropriate to study weakly interacting systems like π-stacking interacting among the graphene layers in 3D graphite, and gave binding energies very close to the experimental results [27]. Many previous works have proven that LDA describes accurately the properties of carbon nanotubes and their interactions with gas molecules. Before working on any new systems, the calculation method used in this work was tested on a well-known system. The interaction of (6, 6) SWNT with benzene has been extensively studied by many groups, hence it was used as a benchmark to test the reliability of our simulation. The adsorption energy of benzene on (6, 6) SWNT has been reported to be -0.10 eV by simulation using CASTEP [28], and -0.19 eV using SIESTA [27]. Our simulation gave an adsorption energy of -0.11 eV, which is consistent with the previous reports. Furthermore, test calculation shows that using a higher cut-off energy (380 eV) or a larger vacuum gap (14 Å) between the graphene sheets has little effect to the simulation results. Therefore, our calculation method is believed to be reliable.

The electron transport calculations were performed using the Atomistix ToolKit (ATK) 2.0.4 package [29], which implements DFT-based real-space, nonequilibrium Green's function (NEGF) formalism [30-32]. The mesh cutoff was chosen as 200 Ry to achieve a reasonable balance between the calculation efficiency and accuracy. The current was calculated by Landauer-Büttiker formula:

$$I = \int_{\mu_L}^{\mu_R} T(E, V_b) dE \tag{2}$$

where $T(E, V_b)$ represents the electronic transport probability, μ_R and μ_L are the chemical potentials of the right and left electrodes, and V_b is the applied bias voltage across the electrodes.

For simplicity, the pristine, boron doped, nitrogen doped and defective graphenes are denoted as P-graphene, B-graphene, N-graphene and D-graphene, respectively, in the following text.

3. Results and discussion

To find the most favorable adsorption configurations, the molecule under investigation is initially placed at different positions above a graphene sheet with different orientations. After full relaxation, the optimized configurations obtained from the different initial states are compared to identify the most energetically stable one. The most stable configurations of the CO, NO, NO_2 and NH_3 molecules on the pristine (P-), boron (B-), nitrogen (N-) and defective (D-) graphene are summarized in figure 1. More detailed information from the simulation of the different molecule-graphene systems, including values of adsorption energy, equilibrium graphene-molecule distance (defined as the center-to-center distance of nearest atoms between graphene and small molecules) and the charge transfer (Mulliken charge), are listed in Table 1. (Calculation results of other less favorable adsorption configurations are available as Supporting Information).

3.1. CO on graphene

Several initial configurations have been considered in order to study the adsorption of CO on the P-graphene. A CO molecule was initially placed above a carbon atom or the center of a six-membered ring (6MR), with the CO molecule oriented perpendicular (with the C or O atom pointing towards the graphene sheet) to the graphene. Several other configurations with the CO molecule placed parallel to the graphene plane were also tested. After full relaxation, a configuration with the adsorbed CO axis aligned parallel to the graphene plane along the axis of two opposite C atoms of the 6MR was found to be the most stable one for the P-graphene. The adsorption energy of this system is -0.12 eV, and the molecule-sheet distance is 3.02 Å (figure 1 a1). The low adsorption energy and long distance indicate a weak interaction. The charge transfer between CO and P-graphene was obtained from Mulliken population analysis (Table 1). For CO on P-graphene, the calculated charges on the C and O atoms of the CO are 0.42 |e| and -0.43 |e|, respectively; while there was no charge on the C atoms of the P-graphene. Meanwhile, a very small charge (0.01 |e|) is transferred from the P-graphene to CO. When adsorbed on B-graphene, CO adoptes a tilted orientation with respect to the plane of the B-containing 6MR, with the C atom close to the B atom. The adsorption energy and charge transfer of the CO on B-graphene system are found to be -0.14 eV and -0.02 |e|, respectively. The CO on

N-graphene system shows very similar adsorption energy of -0.14 eV to the CO on B-graphene system and no charge transfer. The above adsorption energies values suggest that CO can not distinguish p and n type dopants on graphene, which is different from previous report on CO-nanotube interaction [12].

For the D-graphene, the configuration with CO tilted with respected to the graphene plane and the carbon atom pointing towards the vacancy is found to be the most favorable one. The calculation indicates that the graphene carbon atom close to the vacancy defect provides a stronger binding site for the CO molecule than those further away from the vacancy. The minimum atom to atom distance between the CO and the D-graphene is 1.33 Å. This distance is in fact close to the bond length of a C-C double bond and is much shorter than that of the other three types of graphenes, which are 3.02 (P-graphene), 2.97 (B-graphene) and 3.15 (N-graphene) Å (figure 1 a1-3), respectively. The adsorption energy of CO on the D-graphene can reach -2.33 eV, which is more than one magnitude higher than that of the pristine and doped graphenes.

The electronic total charge density plot for the CO on P-graphene is compared with that of the CO on D-graphene, as shown in figure 2. No electron orbital overlap between CO molecule and the P-graphene is observed in the CO on P-graphene system in figure 2(a). In contrast, figure 2(b) shows that the electronic charge plot of CO and the D-graphene are strongly overlapped, leading to more orbital mixing and a larger charge transfer. The electronic total charge density plots for the CO on B-graphene and CO on N-graphene (available in Supporting Information) show similar features with that of the CO on P-graphene, in which no electron density overlap is observed. The total charge density analysis illustrates that only weak physisorption takes place between the CO and P-, N- and B-graphenes, while the vacancy on the D-graphene provides strong chemisorption binding sites for the CO. As the strong orbital overlap between CO and the D-graphene is expected to bring significant change to the electronic properties of the graphene, the D-graphene is expected to be more suitable for sensing CO than the P- and B-, N-graphenes.

3.1.1. NO on graphene

Similarly, the NO molecule was initially placed on the various sites of the four graphenes with different orientations to find the optimal adsorption configurations. The favorable configurations of NO on the different graphenes are similar to the CO on graphene systems, i.e. the N atom adopts similar positions like the C atoms in the CO systems. The only exception occurs on the N-graphene. For the CO on N-graphene, the CO molecule takes an orientation with its C atom pointing at the N atom of the N-graphene; while in the NO on N-graphene, the O atom in the NO molecule is more close to N atom of the N-graphene. The adsorption of NO on the P-graphene is the least exothermic (-0.30 eV), and the molecule-sheet distance is 2.43 Å (figure 1 b1), indicating that the NO is physisorbed on the P-graphene. This result is similar to the recent reports of NO adsorption on carbon nanotube[33, 34]. In the case of B-graphene, the strong interaction between the B and NO leads to a much stronger adsorption energy (-1.07 eV) and the formation of a tight B-N bond (bond distance 1.99 Å), accompanied with an apparent charge transfer of 0.15 |e| from NO to graphene sheet. For the N-graphene, the adsorption energy is -0.40 eV, and the closest distance is 2.32 Å. The D-graphene shows the highest affinity to NO, which gives a -3.04 eV adsorption energy, and the NO-graphene distance is only 1.34 Å (figure 1 b4), revealing the occurrence of a strong chemisorption.

3.1.2. NO_2 on graphene

Different configurations of the triangular shaped NO_2 molecule adsorbed onto the graphene sheets were investigated for a complete understanding of the interaction between NO_2 and different graphenes. Three major possible adsorption configurations were studied, which is similar to the previous studies on the adsorption of NO_2 on carbon nanotubes [13], including that the NO_2 molecule

bonded to the sheet surface with nitrogen end (referred to as nitro configuration), bonded via one oxygen end (referred to as nitrite configuration) and bonded with both oxygen ends (referred to as the cycloaddition configuration). The cycloaddition configuration on P-graphene gives rise to an adsorption energy of -0.48 eV, which is higher than the adsorption energy of the nitro configuration (-0.39 eV) or the nitrite configuration (-0.45 eV). The result is readily understood as that the cycloaddition configuration favors the interaction between the electron rich oxygen atoms and the carbon atoms on the graphene. Meanwhile, a large charge transfer (0.19|e|) from the graphene to NO_2 was observed, confirming that the NO_2 acts as an electron accepter. Given the fact that the adsorption energy is often overestimated at LDA level, the calculated adsorption energy (-0.48 eV) is in a good agreement with the experimentally determined physisorption energy (-0.40 eV) [35] and the adsorption energy (-0.50 eV) for NO_2 on carbon nanotube in theory [34]. On the B-graphene, the nitro configuration gives the stronger interaction than the other configurations. The interaction between the B and N atom leads to a high adsorption energy (-1.37 eV) and the formation of tight B-N bond (bond distance 1.67 Å figure 1 c2), accompanied with an apparent charge transfer of 0.34 |e| from the B-graphene to NO_2. The nitro configuration is also the most favorable one for both the N- and D-graphenes, gives the adsorption energies of -0.98 eV and -3.04 eV, respectively.

3.1.3. NH_3 on graphene

NH_3 molecule shows different adsorption configurations on different graphenes, showing more complicated adsorption mechanism than the other molecules studied above. On the P-graphene, the configuration with the three hydrogen atoms of NH_3 pointing towards graphene plane is the favorable one (figure 1d1), which gives an adsorption energy of -0.11 eV. This result is consistent with previous reports about NH_3 adsorbed on carbon nanotubes (-0.14 eV) and NH_3 adsorbed on graphene (0~-0.17

eV) [15, 22], suggesting a weak interaction between NH_3 and the P-graphene. On the B-graphene, NH_3 is attached to B atom with the N atom pointing at the sheet, which gives adsorption energy of -0.50 eV and a B-N distance of 1.66 Å (figure 1 d2). The adsorption configuration of NH_3 on the N-graphene is similar to that on the P-graphene, which has the hydrogen atoms pointing towards the sheet. However, in the NH_3 on N-graphene system, the N atom is positioned above the N on the N-graphene; while in the NH_3 on P-graphene system, the N is positioned above the 6MR centre. The calculated adsorption energy of NH_3 on the N-graphene is -0.12 eV, indicating the weak physisorption nature. The adsorption of NH_3 on the D-graphene is slightly stronger, which has an adsorption energy of -0.24 eV and little charge transfer. The adsorption energy of NH_3 on the B-graphene (-0.50eV) is much higher than that on the other three graphenes, which is attributed to the strong interaction between the electron-deficient B atom and the electron-donating N atom of NH_3. It is also found that the B-graphene undergo an obvious distortion upon NH_3 adsorption (figure 1 d2), indicating that the B site is transformed from sp^2 hybridization to sp^3 hybridization [15]. The B-N distance (1.66 Å) is very close to the B-N bond length in BH_3NH_3 (1.6576 Å) [36], confirming the formation of covalent bond between the NH_3 and the B-graphene. This strong interaction is also evident in the electronic total charge density of the NH_3 on B-graphene system, which shows large electron density overlap (shown in the Supporting Information).

The interaction between adsorbed molecules and graphenes is expected to alter the electronic structure of the graphenes, which could be reflected by the change in electric conductance of the graphenes Strong interaction could bring about significant conductivity change, which is beneficial for sensing applications. The above calculation results suggest that the P-graphene has weak interactions with all the four gas molecules. Introducing dopant and defect to the graphene

significantly increases the molecule-graphene interaction. Based on above analysis, it is predicted that the B- and D-graphenes are more suitable for gas sensing applications, since they have stronger interactions with the four small molecules than the P- and N-graphenes. More specifically, it is expected that the D-graphene shows the highest sensitivity towards CO, NO and NO_2, while B-graphene is the best choice for sensing NH_3.

3.2. The density of states of molecule-graphene system

To verify the effects of the adsorption of small molecules on the graphenes' electronic properties, the total electronic densities of states (DOS) of the molecule-graphene adsorption systems are calculated, and figure 3 shows the DOS for some representative systems. The above calculations on the adsorption energies have suggested that the CO on P-, B-graphenes and NH_3 on N-graphene systems have weak interactions between the molecules and the graphenes. Such weak interactions are also evident in their DOS structures (figure. 3a-c), which show little change after the adsorption. For example, the DOS of CO on P-graphene and CO on B-graphene are similar to that of the P- and B-graphenes, respectively. The contribution of the CO electronic levels to the total DOS for both systems is localized between -10.0 and -2.6 eV in the valence bands and around 2.5 eV in the conduction bands, which are far away from the Femi level. Similarly, the contribution of the NH_3 electronic level in the NH_3 on N-graphene is localized at -2.3 eV (valence bands) and 2.5 eV (conduction bands), which are also far away from the Fermi level.

In contrast, figure 3d-f shows the DOS of CO on D-graphene, NO on B-graphene and NO_2 on N-graphene are drastically changed from those of the corresponding graphenes due to strong molecule-graphene interactions. Compared with the P-graphene, the DOS of D-graphene shows a large peak appearing just above the Femi level. This peak indicates that the system is strongly

metallic, and a significant increase in conductivity compared with the P-graphene is expected. After the chemisorption of CO molecule, the system becomes more semiconductor like, with a drop of the DOS near the Femi level. Consistent with the adsorption energy values, the DOS analysis also indicates that the interaction between CO and the D-graphene is stronger than that with the pristine one. Such an enhancement in interaction can be directly associated with the rearrangement of the defective sheet structure in the presence of the CO. It is noted that the adsorption of CO onto the D-graphene causes the major band features moved towards higher energy; in other words, the Fermi level shifted towards lower energy.

The adsorption of NO onto B-graphene causes a clear increase of the DOS in the region just above the Fermi level, which is also expected to increase the conductance. Meanwhile, the Fermi level shifts slightly towards higher energy after the adsorption. It is understood that the B dopant introduces electronic holes to the graphene, which generates a p-type semiconductor. When B-graphene interacts with an electron-rich NO molecule, a large charge transfer to the B-graphene occurs, which dramatically enhances the conductivity of the NO on B-graphene system. For the NO_2 on N-graphene, the strong interaction causes a dramatic increase of the DOS in both sides near the Femi level. The change in the DOS, especially the area near Fermi level, is expected to bring about obvious change in the corresponding electronic properties. Therefore, it is concluded from figure 3 that the D-graphene, B-graphene and N-graphene are suitable for sensing application to CO, NO and NO_2, respectively.

The I-V curves of molecule on graphene

To quantitatively evaluate the gas sensing properties of the graphenes, the electron transport properties of the different graphenes are simulated using NEGF methods. The simplest type chemical sensing transducer is a resistance sensor, in which the resistance of the sensing materials upon the

adsorption of chemicals is detected. Graphene-based resistance sensors are simulated using a model consisting of a graphene sheet contacted by two graphene electrodes (figure 4a). We have calculated a series of current verses voltage (I-V) curves for such graphene junction with and without the adsorption of different molecules. The simulated I-V curves for the P-graphene and B-graphene before and after NO_2, NH_3 adsorption are illustrated in figure 4b and 4c. The I-V curve of the P-graphene exhibits clear non-linear behavior. The B-graphene is about 3 times more conductive than the P-graphene due to the increased hole-type charge carriers, which confirms our previous finding in the DOS analysis (figure 3e). After NO_2 adsorption, a slight current increase is observed for the NO_2 on P-graphene. In contrast, dramatic increase of current is observed for the NO_2 on B-graphene, indicating a much higher sensitivity. After normalized against the intrinsic conductivity of the corresponding graphenes (figure 4d), the sensitivity of B-graphene to NO_2 is found to be dependent on the bias voltage, and a high sensitivity bias window between 0.8 and 1.2 V are visible. At the optimum bias voltage of 1.0 V, the B-graphene shows a sensitivity nearly two orders of magnitude higher than that of the P-graphene (figure 4d). The B-graphene is less sensitive to NH_3 than to NO_2, but still shows one order of magnitude higher sensitivity than the P-graphene when the bias voltage is higher than 1.0 V.

Concerns for practical application

Though the above calculation results suggests that the doped and defective graphenes exhibit much improved sensing properties than the pristine graphene, it worth noting that the strong binding between the modified graphenes and certain molecules may also brings about some serious drawbacks. For example, strong binding implies that the desorption of the gas molecules from the doped and defective graphenes could be difficult and the devices may suffer from longer recovery time.

Novoselov *et al.*[4] have demonstrated that the graphene-sensor could be regenerated to its initial state within 100-200 seconds by annealing at 150 °C in vacuum or short UV irradiation. However, much longer recovery time is expected if the adsorption energy is significantly increased. According to the conventional transition state theory, the recovery time τ can be expressed as:

$$\tau = \nu_0^{-1} \mathrm{e}^{(-E_\mathrm{B}/K_\mathrm{B}T)} \tag{3}$$

where T is temperature, K_B the Boltzmann's Constant and ν_0 the attempt frequency. Increasing the adsorption energy E_ad will prolong the recovery time in an exponential manner. It is estimated that in a strong binding case, like the NO_2 on D-graphene, the recovery time could be in the order of 10^{10} hours at 600K, which is obviously not acceptable from any practical application. The desorption of the small molecules from graphene surface may be assisted by UV irradiation [37] or electric field [38], which has been exploited to clean up adsorpants on carbon nanotubes or metals. But the effectiveness of these cleaning methods has not been fully investigated on graphene devices. Therefore, before any innovative cleaning method is uncovered, the graphene-based sensing devices are more likely to find applications as highly sensitive irreversible sensors rather than ideal reversible sensors. As last, we note that graphene-based sensor is still in its early stage and much work is needed before it may compete with many currently available sensors. Fundamental understanding of the binding pehenomena of small molecules on graphene are essential to explore this new field.

4. Conclusions

In summary, the adsorption of CO, NO, NO_2 and NH_3 on the P-, B-, N-, and D-graphenes were investigated. Four molecules show physisorption on the P-graphene with low adsorption energies and little charge transfer, which suggest that the un-modified graphene is not an ideal material for gas

sensing. The N-graphene shows weak interactions with CO, NO and NH_3, but strong binding with NO_2 with an adsorption energy of -0.98 eV. The B-doping appears to enhance the interactions between the graphene and NO, NO_2 or NH_3. The defective graphene strongly interacts with CO, NO and NO_2 but weakly with NH_3. The I-V simulation on graphene-based electronic junctions illustrates that the sensitivity of B-graphene to NO_2 molecule could be two orders of magnitude higher than that of the P-graphene. This work demonstrates that the sensitivity and selectivity of graphene-based gas sensors could be significantly improved by introducing dopant or defect into the graphenes.

Acknowledgements: The authors are grateful to the financial support from the program for New Century Excellent Talents in University (NCET), National Natural Science Foundation of China (NSFC. 20503011, 20621091), fund from the Ministry of Education of China (SRFDP. 20050730007, 106152) and support from the Chunhui project and "111" project. The simulation work was conducted in the High Performance Computing Center of Lanzhou University.

References

[1] Novoselov K S, Geim A K, Morozov S V, Jiang D, Zhang Y, Dubonos S V, Grigorieva I V and Firsov A A 2004 *Science* **306** 666

[2] Stankovich S, Dikin D A, Dommett G H B, Kohlhaas K M, Zimney E J, Stach E A, Piner R D, Nguyen S T and Ruoff R S 2006 *Nature* **442** 282

[3] Watcharotone S *et al* 2007 *Nano Lett.* **7** 1888

[4] Schedin F, Geim A K, Moeozov S V, Hill E W, Blake P, Katsnelson M I and Novoselov K S 2007 *Nat. Mater.* **6** 652

[5]Barbolina I I, Novoselov K S, Morozov S V, Dubonos S V, Missous M, Volkov A O, Christian D A, Grigorieva I V and Geim A K 2006 *Appl. Phys. Lett.* **88** 013901

[6] Tombros N, Jozsa C, Popinciuc M, Jonkman H T and Wees B J v 2007 *Nature* **448** 571

[7] Di C-a, Wei D, Yu G, Liu Y, Guo Y and Zhu D 2008 *Adv. Mater.* **20** 3289

[8] Wang X, Zhi L and Mullen K 2007 *Nano Lett.* **8** 323

[9] Becerill H A, Mao J, Liu Z, Stoltenberg R M, Bao Z and Chen Y 2008 *ACS Nano* **2** 463

[10] Geim A K and Novoselov K S 2007 *Nat. Mater* **6** 183

[11] Kong J, Franklin N R, Zhou C, Chapline M G, Peng S, Cho K and Dai H 2000 *Science* **287** 622

[12] Peng S and Cho K 2003 *Nano Lett.* **3** 513

[13] Yim W L, Gong X G and Liu Z F 2003 *J. Phys. Chem. B* **107** 9363

[14] Seo K, Park K A, Kim C, Han S, Kim B and Lee Y H 2005 *J. Am. Chem. Soc.* **127** 15724

[15] Bai L and Zhou Z 2007 *Carbon* **45** 2105

[16] Leenaerts O, Partoens B and Peeters F M 2008 *Phys. Rev. B* **77** 125416

[17] Ao Z M, Yang J, Li S and Jiang Q 2008 *Chem. Phys. Lett.* **461** 276

[18] Kang H S 2005 *J. Am. Chem. Soc.* **127** 9839

[19] Fagan S B, Filho A G S, Lima J O G, Filho J M, Ferreira O P, Mazali I O, Alves O L and Dresselhaus M S 2004 *Nano Lett.* **4** 1285

[20] Zhang Y, Zhang D and Liu C 2006 *J. Phys. Chem. B* **110** 4671

[21] Chang H, Lee J D, Leeb S M and Lee Y H 2001 *Appl. Phys. Lett.* **79** 3863

[22] Charles W. Bauschlicher J and Ricca A 2004 *Phys. Rev. B* **70** 115409

[23] Peng S and Cho K 2000 *Nanotechnology* **11** 57

[24] Zhao J, Buldum A, Han J and Lu J 2002 *Nanotechnology* **13** 195

[25] Milman V, Winkler B, White J A, Pickard C J, Payne M C, Akhmatskaya E V and Nobes R H 2000 *J. Quantum Chem.* **77** 895

[26] Zhao Q, Nardelli M B, Lu W and Bernholc J 2005 *Nano Lett.* **5** 847

[27] Tournus F and Charlier J-C 2005 *Phys. Rev. B* **71** 165421

[28] Lu J *et al* 2006 *J. Am. Chem. Soc.* **128** 5114

[29] Taylor J, Guo H and Wang J 2001 *Phys. Rev. B* **63** 245407

[30] Brandbyge M, Mozos J-L, Ordejón P, Taylor J and Stokbro K 2002 *Phys. Rev. B* **65** 165401

[31] Soler J M, Artacho E, Gale J D, García A, Junquera J, Ordejón P and Sánchez-Portal D 2002 *J. Phys.: Condens. Matter* **14** 2745

[32] Brandbyge M, Kobayashi N and Tsukada M 1999 *Phys. Rev. B* **60** 17064

[33] Wang R, Zhang D, Sun W, Han Z and Liu C 2007 *Journal of Molecular Structure: THEOCHEM* **806** 93

[34] Peng S, Cho K, Qi P and Dai H 2004 *Chem. Phys. Lett.* **387** 271

[35] Sjövall P, So S K, Kasemo B, Franchy R and Ho W 1990 *Chem. Phys. Lett.* **172** 125

[36] Dixon D A and Gutowski M 2005 *J. Phys. Chem. A* **109** 5129

[37] Chen R, Franklin N, Kong J, Cao J, Tombler T, Zhang Y and Dai H 2001 *Appl. Phys. Lett.* **79** 2258

[38] Hyman M P and Medlin J W 2005 *J. Phys. Chem. B* **109** 6304

Table and Figure Captions

Table 1 Adsorption energy (E_{ad}), equilibrium graphene-molecule distance (d) (defined as the shortest atom-to-atom distance), and Mulliken charge (Q) of small molecules adsorbed on different graphene sheets.

Figure 1. Schematic view of the favorable adsorption configurations of the CO, NO, NO_2 and NH_3 molecules on the P-, B-, N-, and D-graphenes. C, B, N, O and H atoms are shown as grey, pink, blue, red and white, respectively.

Figure 2. Electronic total charge densities for the adsorption adducts of (a) CO on P-graphene and (b) CO on D-graphene.

Figure 3. Total electronic density of states for P-, B-, N- and D-graphene (black curves) and molecule-graphene systems (red curves) calculated for the corresponding configurations shown in Figure 1 (a1, a2, d3, a4, b2 and c3). The Fermi level is set to zero.

Figure 4. (a) A schematic illustration of the graphene-based chemical sensor for detecting small gas molecules. (b) A comparison of the I-V curves of the devices based on P-graphene, NO_2 on P-graphene, B-graphene and NO_2 on B-graphene. (c) The I-V curves of the devices based on P-graphene, NH_3 on P-graphene, B-graphene and NH_3 on B-graphene. (d) The normalized I-V curves of the P-graphene and B-graphene. It should be noted that the I-V curves in (b) and (c) are offset for 0.02×10^{-6} A from each other, while the curves in (d) are offset for 4 from each other for clarity.

System	EB_{ad}	d (Å)	Q (e)[a]
CO on P-graphene	-0.12	3.02	-0.01
NO on P-graphene	-0.30	2.43	0.04
NO_2 on P-graphene	-0.48	2.73	-0.19
NH_3 on P-graphene	-0.11	2.85	0.02
CO on B-graphene	-0.14	2.97	-0.02
NO on B-graphene	-1.07	1.99	0.15
NO_2 on B-graphene	-1.37	1.67	-0.34
NH_3 on B-graphene	-0.50	1.66	0.40
CO on N-graphene	-0.14	3.15	0
NO on N-graphene	-0.40	2.32	0.01
NO_2 on N-graphene	-0.98	2.87	-0.55
NH_3 on N-graphene	-0.12	2.86	0.04
CO on D-graphene	-2.33	1.33	0.26
NO on D-graphene	-3.04	1.34	-0.29
NO_2 on D-graphene	-3.04	1.42	-0.38
NH_3 on D-graphene	-0.24	2.61	0.02

[a]Q is defined as the total Mulliken charge on the molecules, and negative number means charge transfer from graphene to molecule.

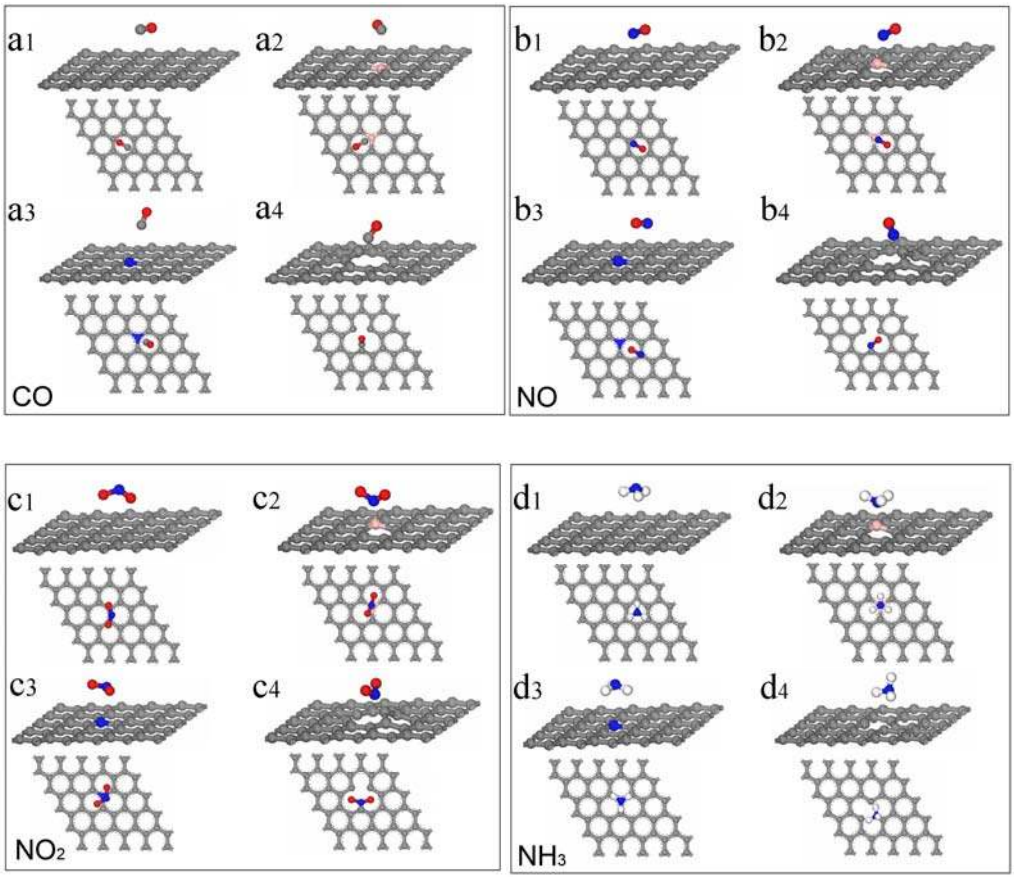

Figure 1 by Y. H. Zhang et. al.

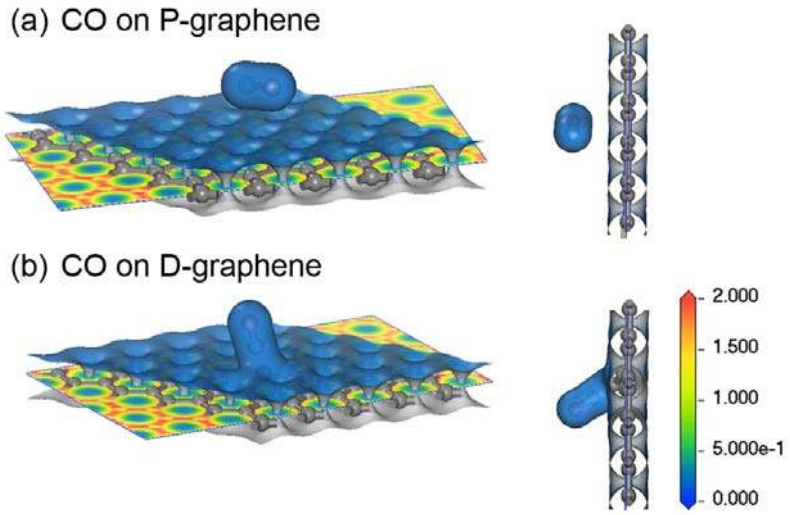

Figure 2 by Y. H. Zhang et. al.

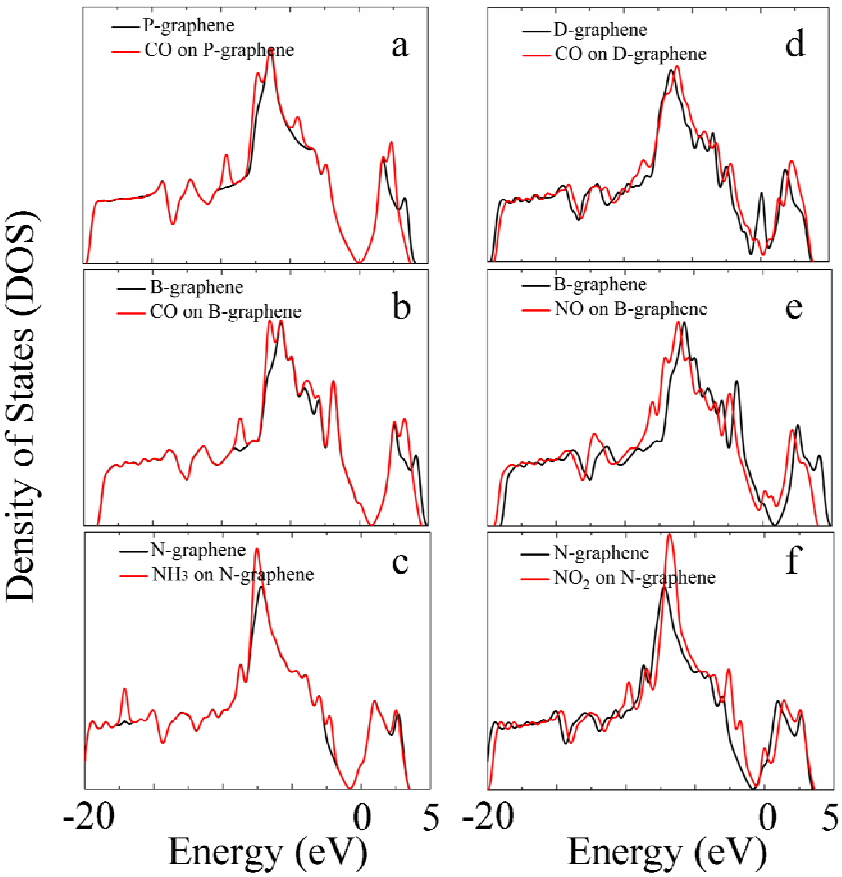

Figure 3 by Y. H. Zhang et. al.

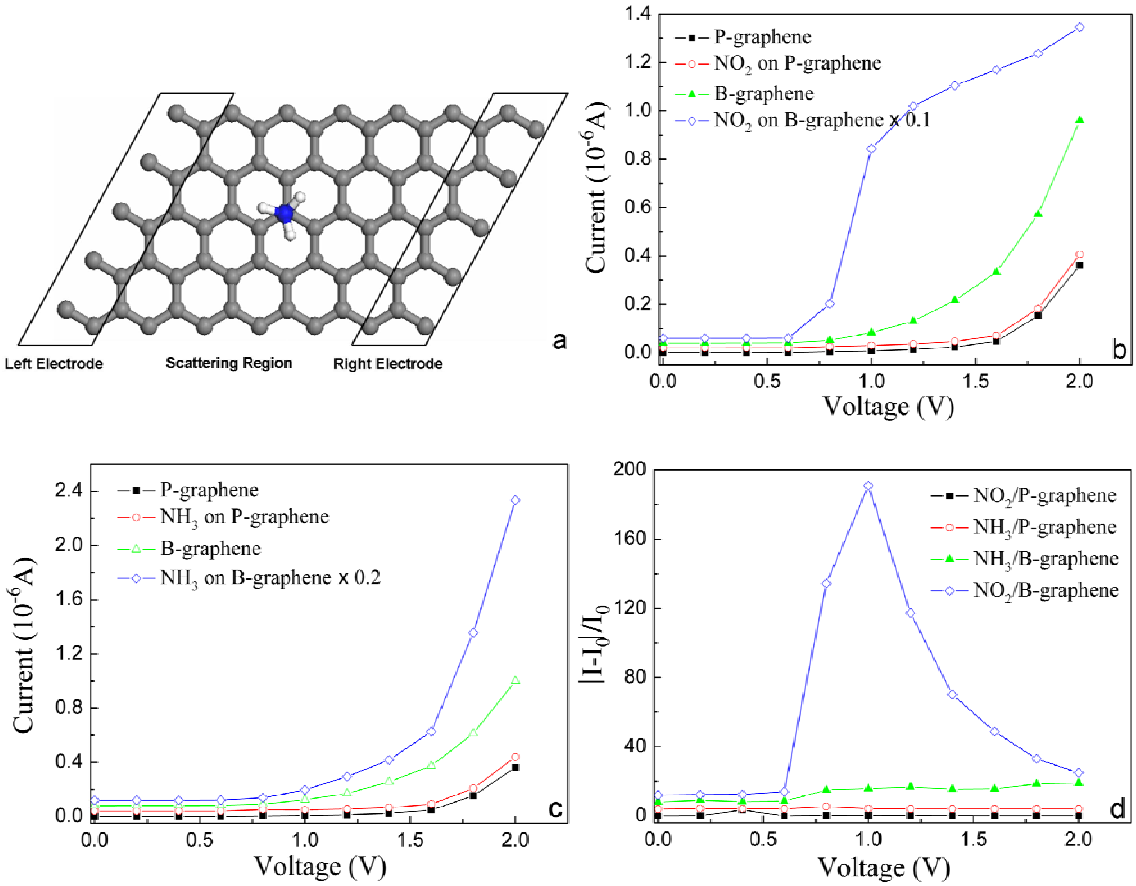

Figure 4 by Y. H. Zhang et. al